A FINITE ELEMENT MODELING COMPARISON OF CRANIOCERVICAL MOTION IN DOWN SYNDROME VERSUS NORMAL AGE-MATCHED CONTROL

Jakob Harley Astin (Benjamin Ellis)
Department of Biomedical Engineering

Abstract:

The craniocervical junction (CCJ), comprising the base of the skull and the first and second vertebrae in the cervical spine, is a vital junction in keeping the head stable. It is well known that individuals with Down syndrome (DS) commonly have instability in this region of the neck; however, it is unknown whether the shape of the bone or the stiffness of the ligaments in this region is the primary contributor to this. Historically, it is believed that laxity in the ligaments of individuals with DS solely leads to the looser connection seen in these patients. Using finite element modeling, this study attempts to quantify the contribution of bone morphology to this instability.

Two CCJ finite element models (FEMs) were generated from age-matched pediatric patients, one with DS and one a normal control (Fig. 1). Computed tomography scans of the patients were used to create shells of the desired bony structures via segmentation, while soft tissues and ligamentous structures were added based on bony landmarks. Ligament stiffness values were assigned using published adult ligament stiffness properties. Range of motion (ROM) testing determined that model behavior most closely matched pediatric cadaveric data when ligament stiffness values were scaled down to 25% of those found in adults (Fig. 2). These values, along with those assigned to the other soft-tissue materials, were identical for each model to ensure that the only variable between the two was the bone morphology.

The FEMs were then subjected to three types of simulations to assess their rotational ROM, anterior-posterior (A-P) translation, and axial tension. In ROM testing, a torque was applied to the skull to rotate it in all the cardinal directions of movement (flexion/extension, lateral bending, and axial rotation), and the resulting rotation was recorded as an Euler angle in relation to the base of the CCJ. During A-P translation, forces were applied to the skull to push it forward and backward, and the resulting displacement was recorded. In axial tension, the skull was displaced upwards by a set amount, the force required to do so was recorded for each model, and a structural stiffness was calculated.

The DS model exhibited more laxity than the normal model at all levels for all of the cardinal ROMs (Fig. 3) and A-P translation (Fig. 4). The flexion/extension, lateral bending, axial rotation, and A-P translation predicted by the DS model were 40.7%, 52.1%, 26.1%, and 39.8% larger than the normal model, respectively. When simulating axial tension, however, the DS and normal models' soft-tissue structural stiffness was nearly identical (Fig. 5), indicating that the ligaments in these FEMs behaved in the same manner.

The increased laxity exhibited by the DS model in the cardinal ROMs and A-P translation, along with the nearly identical soft-tissue structural stiffness exhibited in axial tension, calls into question the previously held notion that ligamentous laxity is the sole explanation for craniocervical instability in DS.
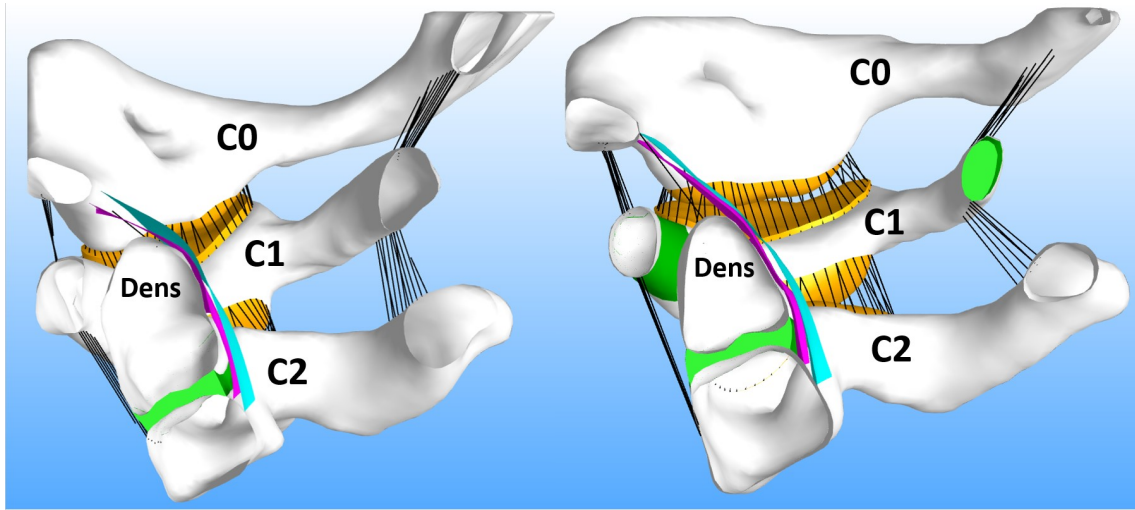
Figure 1. FEMs of the CCJ of a 3-year-old normal girl (left) and a 3-year-old boy with DS (right). The images are taken from PostView, where the models have been sliced along their x-axis to show a cross-sectional view. In these models, TM is colored cyan, TL pink, facets orange, spring elements black, and cartilage green.
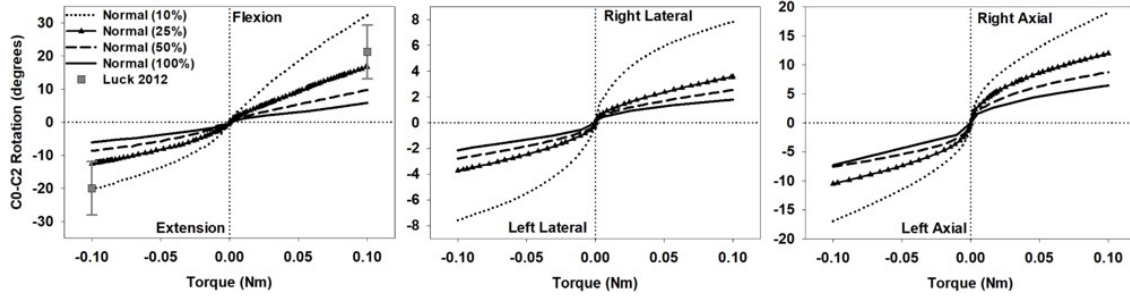
Figure 2. Spring stiffness assessment using the normal model tested in flexion-extension (left), lateral bending (middle), and axial rotation (right) at 100%, 50%, 25%, and 10% of the adult ligament stiffness values available in the literature.
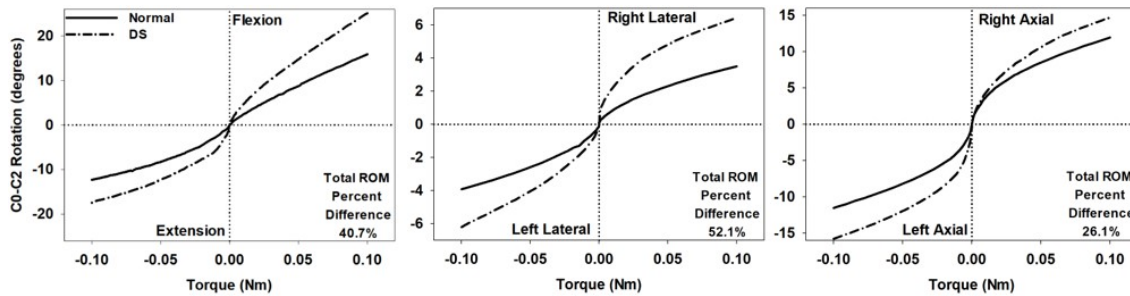

Figure 3. DS (dotted line) versus normal FEM (solid line) predictions of ROM in flexion-extension (left), lateral bending (middle), and axial rotation (right).
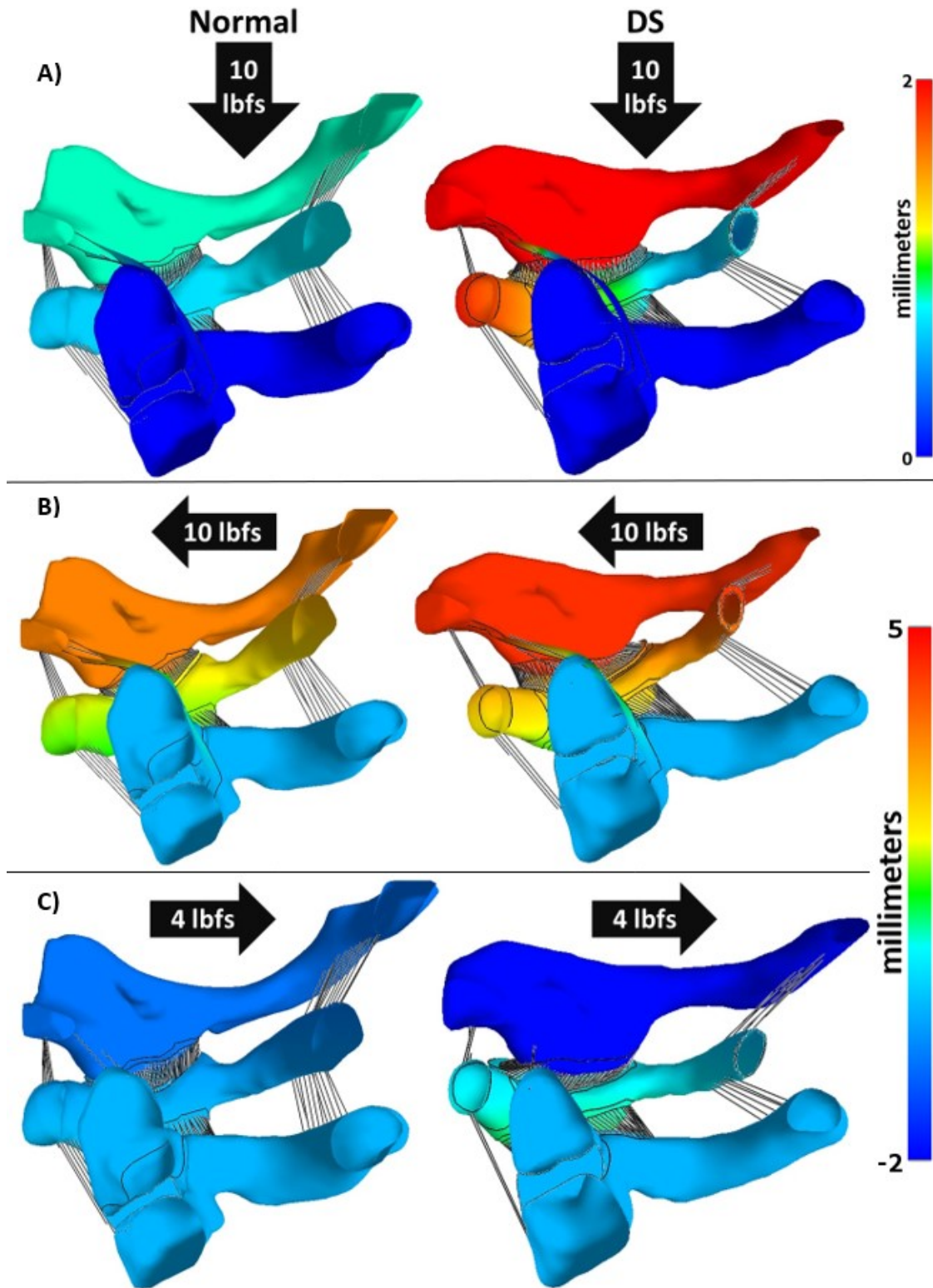
Figure 4. DS (right) versus normal (left) FEM predictions of A-P translation: a downward load was applied and maintained (A), followed by anterior (B) and posterior (C) loads.
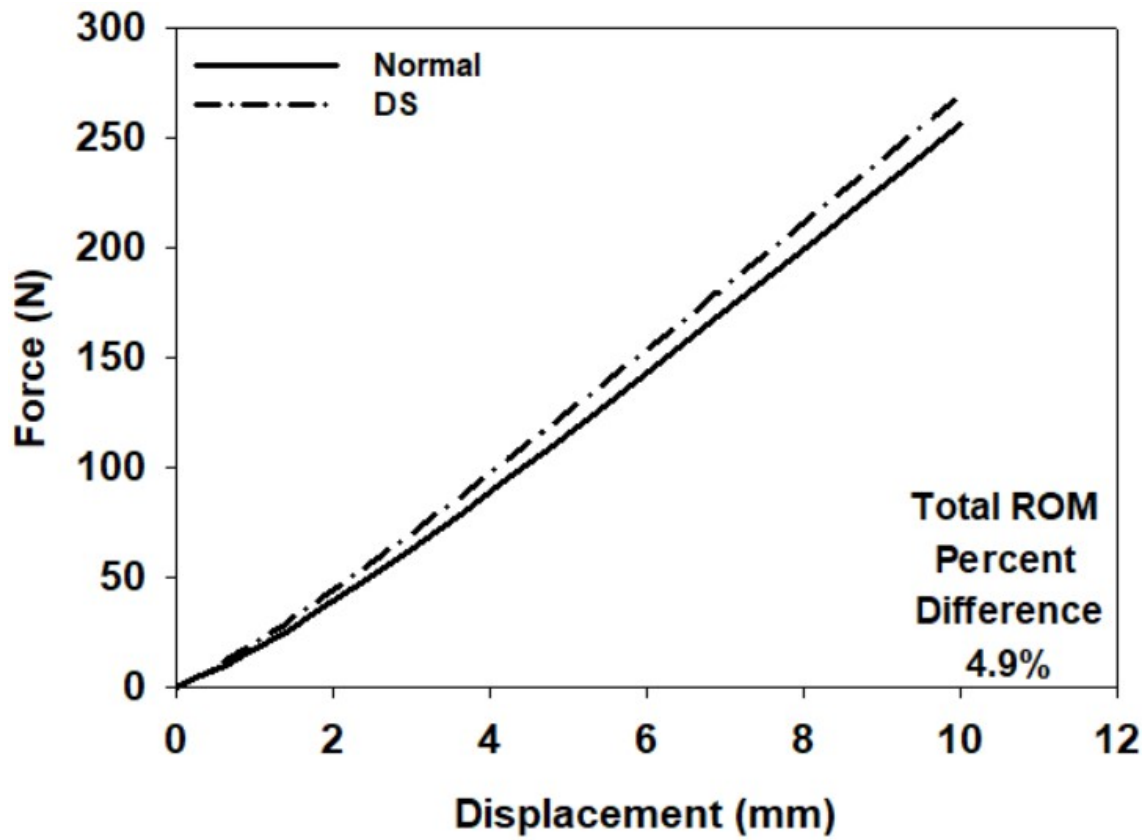
Figure 5. DS versus normal FEM predictions of soft-tissue structural stiffness in axial tension.